Face to phase: pitfalls in time delay estimation from coherency phase

**S. Floor Campfens · Herman van der Kooij ·
Alfred C. Schouten**

Abstract Coherency phase is often interpreted as a time delay reflecting a transmission delay between spatially separated neural populations. However, time delays estimated from corticomuscular coherency are conflicting and often shorter than expected physiologically. Recent work suggests that corticomuscular coherence is influenced by afferent sensory feedback and bidirectional interactions. We investigated how bidirectional interaction affects time delay estimated from coherency, using a feedback model of the corticomuscular system. We also evaluated the effect of bidirectional interaction on two popular directed connectivity measures: directed transfer function (DTF) and partial directed coherence (PDC). The model is able to reproduce the range of time delays found experimentally from coherency phase by varying the strengths of the efferent and afferent pathways and the recording of sensory feedback in the cortical signal. Both coherency phase and DTF phase were affected by sensory feedback, resulting in an underestimation of the transmission delay. Coherency phase was altered by the recording of sensory feedback in the cortical signals and both measures were affected by the presence of a closed loop feedback system. Only PDC phase led to the correct estimation of efferent transmission delay in all simulated model configurations. Coherency and DTF phase should not be used to estimate transmission delays in neural networks as the estimated time delays are meaningless in the presence of sensory feedback and closed feedback loops.

Keywords Coherence · DTF · PDC · Time delay · Phase · Sensory feedback

1 Introduction

Correlation analysis between signals, e.g. coherence, is widely used in neuroscience to detect connectivity between spatially separated populations of neurons (Varela et al. 2001; Horwitz 2003; Fries 2005; Stam and van Straaten 2012). The (magnitude squared) coherence, a frequency domain measure of correlation, varies between zero (no correlation) and one (linear, noise free correlation) (Pintelon and Schoukens 2001). Coherence is the magnitude squared of the (complex) coherency where coherency phase describes the relative timing between the two signals as a function of frequency (Halliday et al. 1995). The coherency phase is often used to indicate which signal is leading and to get an estimate of the transmission delay (Mima et al. 2000; Tallon-Baudry et al. 2001; Riddle et al. 2004; Nolte et al. 2004; Witham et al. 2007).

Corticomuscular coherence (CMC) in the beta band demonstrates connectivity between the cortex (activity recorded with EEG and MEG) and the spinal motor neurons (activity recorded with EMG). Typically a proportional

S. F. Campfens (✉) · H. van der Kooij · A. C. Schouten
Laboratory of Biomechanical Engineering,
MIRA Institute of Biomedical Engineering
and Technical Medicine, University of Twente,
PO box 217, 7500 AE, Enschede, the Netherlands
e-mail: s.f.campfens@utwente.nl

S. F. Campfens
Clinical Neurophysiology Chair, MIRA Institute of Biomedical
Engineering and Technical Medicine, University of Twente,
Enschede, the Netherlands

H. van der Kooij · A. C. Schouten
Department of Biomechanical Engineering,
Delft University of Technology,
Delft, the Netherlands

phase-frequency relation is found, suggesting a transmission delay, which is estimated from the slope of the phase-frequency relation (Brown et al. 1998; Mima et al. 2000; Gross et al. 2000; Grosse et al. 2003; Riddle and Baker 2005; Baker et al. 2006; Williams et al. 2009; Petersen et al. 2012). This estimated time delay can be compared with the delay of for example a motor evoked potential. Some studies found good agreement between these different methods to estimate the efferent transmission delay (Gross et al. 2000; Petersen et al. 2012). Others report shorter (Brown et al. 1998; Grosse et al. 2003; Riddle and Baker 2005) or non-meaningful, i.e. zero (Halliday et al. 1998; Riddle and Baker 2005), time delays based on phase analysis.

Over the last decade, evidence is accumulating that CMC is affected by the properties of the efferent and afferent pathways and that there is a bidirectional connectivity between cortical and peripheral activity in the corticomuscular system (Pohja and Salenius 2003; Riddle and Baker 2005; Williams et al. 2009; Witham et al. 2011). The bidirectional connectivity might underlie the low agreement between transmission delays that are estimated from coherency phase (Williams et al. 2009; Witham et al. 2011; Schouten and Campfens 2012). One scenario for the bidirectional connectivity is the presence of a closed loop feedback system where the ongoing motor activity is modulated by the sensory feedback signals. Another scenario would be that sensory feedback signals are present in the recorded cortical activity, possibly due to afferent projections to the motor cortex or due to volume conduction.

Here, we investigated how the coherency phase and estimated time delay are affected by bidirectional connectivity due to the presence of a closed feedback loop, sensory feedback in the recorded cortical signal, or both. We also estimated time delays based on the two most popular directed connectivity measures based on Granger causality: the Directed Transfer Function (DTF, Kamiński and Blinowska 1991) and Partial Directed Coherence (PDC, Baccalá and Sameshima 2001).

2 Methods

We estimated time delays from the phase of connectivity measures (coherency, DTF and PDC) using model simulations of the corticomuscular system.

2.1 Model of corticomuscular system

The corticomuscular system (Fig. 1) was modeled as a feedback system with two inputs: cortical motor drive (MD) and motor noise (MN). The efferent and afferent pathways were both modeled as a variable gains (K) and fixed time delays (TD). The values for the time delays were taken from literature where the response to external stimulation is taken as an estimate of transmission delay. The efferent delay was
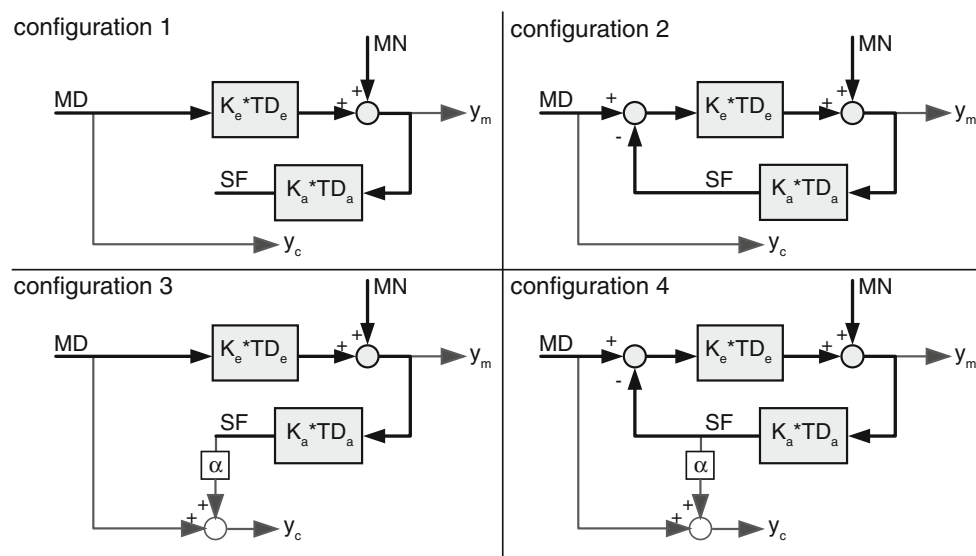
Fig. 1 Overview of the four configurations of the corticomuscular system model. The efferent and afferent pathways are modeled as neural gains (K_E and K_A) and neural time delays (TD$_E$ and TD$_A$). The model receives two inputs: a motor drive (MD) and motor noise (MN). The two output signal represent muscle activity (y_m) and cortical activity (y_c). In configurations 2 and 4 (right column) the system forms a closed feedback loop where the sensory feedback modulates the motor activity (input of the efferent pathway). In configurations 3 and 4 sensory feedback (SF) is recorded in cortical signal. The magnitude of SF in the cortical signal is determined by α

set at 18ms based on motor evoked potentials at the wrist (Rothwell et al. 1991). The afferent, proprioceptive, delay was set at 25ms based on sensory evoked potentials (Abbruzzese et al. 1985).

Two settings for the cortical signal and two different structures for the corticomuscular system were combined, resulting in four model configurations (see Fig. 1). In the first two configurations the cortical signal reflects the motor drive only (upper row in Fig. 1). In configurations 3 and 4 sensory feedback is present in the cortical signal, where the amount of the sensory feedback signal is varied with α. In the one system structure (configurations 1 and 3, left column in Fig. 1) the sensory feedback signal does not contribute to the motor activity. In the other system structure (configurations 2 and 4, right column in Fig. 1) the sensory feedback signal is fed back and modulates the ongoing motor activity resulting in a closed loop feedback system.

2.2 Model simulations

The model is implemented in Matlab as a discreet state space system. Input signals of the model (MD and MN) were two independent normally distributed white noise signals. For each of the model configurations, the model was simulated for 200s at 1kHz. The model simulations provided the cortical and muscle signal (y_c and y_m respectively) which were used for further analysis.

We investigated the effect of the relative afferent contribution by varying the strength of the afferent pathway while the efferent pathways was kept constant: $K_A = \{0.1, 0.2, \ldots, 0.8\}$; $K_E = 1$. For all combinations of K_E and K_A the total loop gain is smaller than one assuring the model always satisfies the Nyquist stability criterion. The time delays of the efferent and afferent pathway were fixed in all simulations. Furthermore, to investigate the effect of the signal power we made three combinations of input signal variances and α:

- $\sigma^2_{MD} = 1, \sigma^2_{MN} = 0.5, \alpha = 0.25$;
- $\sigma^2_{MD} = 0.5, \sigma^2_{MN} = 1, \alpha = 0.25$ and
- $\sigma^2_{MD} = 0.5, \sigma^2_{MN} = 1, \alpha = 1$.

2.2.1 Coherency

Coherency was calculated following the standard procedures (Rosenberg et al. 1989; Halliday et al. 1995). Signals were segmented in 200 non-overlapping epochs of 1s and transformed to the frequency domain using the fast Fourier transform. Power spectral density ($\Phi_{y_c y_c}$ and $\Phi_{y_m y_m}$) and cross spectral density ($\Phi_{y_c y_m}$) were calculated using

$$\Phi_{y_c y_c}(f) = \frac{1}{N} \sum_{k=1}^{N} Y^*_{c,k}(f) \cdot Y_{c,k}(f) \qquad (1)$$

and

$$\Phi_{y_c y_m}(f) = \frac{1}{N} \sum_{k=1}^{N} Y^*_{c,k}(f) \cdot Y_{m,k}(f) \qquad (2)$$

where $Y_{c,k}(f)$ and $Y_{m,k}(f)$ are the Fourier coefficients at frequency f calculated from the kth segment of y_c and y_m, respectively. The asterisk indicates the complex conjugate and N is the total number of segments (200). The complex valued coherency ($C_{y_c y_m}$) between the cortical and muscle signal was calculated according to

$$C_{y_c y_m}(f) = \frac{\Phi_{y_c y_m}(f)}{\sqrt{\Phi_{y_c y_c}(f)\Phi_{y_m y_m}(f)}}. \qquad (3)$$

We only evaluate coherency phase and not magnitude, as the latter is a measure of the amount of additional independent noise in the signals which is not related to the dynamics between y_c and y_m.

2.2.2 Directed connectivity

Both DTF and PDC are based on a multivariate auto regressive (MVAR) model of the data.

An MVAR model of the form

$$\begin{bmatrix} y_c(n) \\ y_m(n) \end{bmatrix} = \sum_{r=1}^{p} \mathbf{A}_r \begin{bmatrix} y_c(n-r) \\ y_m(n-r) \end{bmatrix} + \begin{bmatrix} \varepsilon_1(n) \\ \varepsilon_2(n) \end{bmatrix} \qquad (4)$$

was fitted to the segmented signals using the freely available ARfit package (Schneider and Neumaier 2001). The 2-by-2 matrix $\mathbf{A}_r$ contains the coefficients that predict the current sample (n) of y_c and y_m from the rth past sample of y_c and y_m. The model order, p, determines how many past samples are included in the prediction of the current sample and was chosen based on the final prediction error criterion (Akaike 1971). The prediction error ε is minimized in the fitting of the coefficients of $\mathbf{A}_r$ of the MVAR model.

Transformation of the MVAR model to the frequency domain yields

$$\begin{bmatrix} Y_c(f) \\ Y_m(f) \end{bmatrix} = \mathbf{H}(f) \begin{bmatrix} E_1(f) \\ E_2(f) \end{bmatrix}, \qquad (5)$$

where $\mathbf{H}(f)$ is the 2-by-2 *transfer function matrix* of the MVAR model. The transfer function matrix is calculated from the Fourier transform of $\mathbf{A}_r$ according to:

$$\mathbf{H}(f) = \left(\mathbf{I} - \sum_{r=1}^{p} \mathbf{A}_r e^{-i2\pi \Delta t f} \right)^{-1}, \qquad (6)$$

where i is the imaginary unit and Δt is the sample time.

The directed transfer function (DTF) is calculated from the MVAR transfer function matrix $\mathbf{H}(f)$, normalizing each

element $H_{i,j}(f)$ to the relevant row of $\mathbf{H}(f)$ (Kamiński and Blinowska [1991](#)):

$$DTF_{ij} = \frac{|H_{ij}(f)|^2}{\sum_{m=1}^{2}|H_{im}(f)|^2}. \tag{7}$$

Similar to how the coherency phase is determined by the phase of $\Phi_{y_c y_m}(f)$, the phase of the DTF is determined by the phase of $H_{i,j}(f)$. The phase of $H_{2,1}$ was used to estimate the time delay between y_c and y_m.

Partial directed coherence (PDC) is calculated directly from the Fourier transform of the matrices $\mathbf{A}_r$:

$$\overline{\mathbf{A}}(f) = \mathbf{I} - \sum_{r=1}^{p} \mathbf{A}_r e^{-i2\pi \Delta t f}. \tag{8}$$

In the calculation of the PDC, each element of $\overline{A}_{i,j}(f)$ in normalized to the relevant column of $\overline{A}(f)$ (Baccalá and Sameshima [2001](#); Florin et al. [2010](#)):

$$PDC_{ij}(f) = \frac{\overline{A}_{ij}(f)}{\sqrt{\sum_{m=1}^{2}|\overline{A}_{mj}|^2}}. \tag{9}$$

The phase of $\overline{A}_{2,1}$ was used to estimate the time delay between y_c and y_m.

2.2.3 Time delay estimation

In experimental studies from literature, the time delay is estimated from the phase slope on frequencies where significant connectivity was found, typically the beta band ($15 - 30$Hz). For the simulations, time delays between the cortical and muscle signal were calculated by fitting a straight line onto the phases of coherency, DTF and PDC in the beta band ($15-30$Hz) (Mima et al. [2001](#)). A negative phase slope indicated that the cortical signal was leading the muscle signal. The slope was divided by $-360°$ to transform the units from $°$/Hz (unit of the slope) to s (unit of time delay). Note

that with this definition a positive value for the time delay indicated that y_c leads y_m.

3 Results

3.1 Coherency phase and time delay

When the corticomuscular system was modeled with an efferent pathway only (configuration 1) the coherency phase was proportionally related to frequency (Fig. [2](#)), as expected. Both when sensory feedback was recorded in the cortical signal (configurations 3 and 4) and when the system formed a closed feedback loop (configurations 2 and 4) the phase had a very different relation with frequency. In these configurations the coherency phase showed fluctuations around the proportional phase frequency relation. The amplitude of the fluctuations increased when K_A was increased (Fig. [2](#)). These fluctuations resulted in a reduced slope of the coherency phase in the beta band and the fitted line has a non-zero intercept, i.e. does not indicate zero degrees at $f = 0$. In configuration 4, increasing the value of K_A even led to a positive slope of the coherency phase in the beta band. Due to the fluctuations in the phase, the slope of the phase-frequency relation is not the same in different frequency bands.

The total transmission delay in the system ($TD_E + TD_A$) determines the period of the fluctuation, i.e. the frequency at which the fluctuating phase crosses the line corresponding to the efferent transmission delay for the second time. The transmission delays of the efferent and afferent pathway add to a total transmission delay of 43ms resulting in a period of the fluctuation of approximately 23Hz. As a result of this fluctuation-period, the phase frequency relation in the beta band can be described by a straight line with non-zero intercept and a slope suggesting a shorter time delay than the

Fig. 2 Coherency phase for the four model configurations and different values of K_A. *Dashed lines* are the straight lines fitted through the phases in the beta band (15–30Hz, grey area), the slope of this line is the estimated time delay
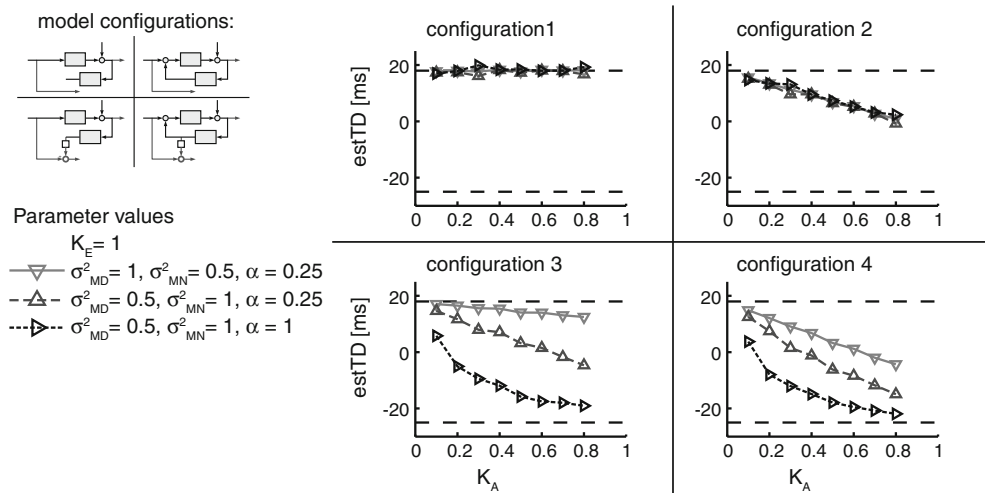

model configurations:
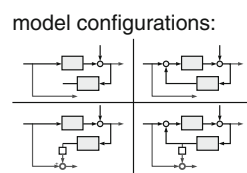
Parameter values:
$\sigma^2_{MD} = 1$
$\sigma^2_{MN} = 0.5$
$\alpha = 0.25$
$K_E = 1$

- $K_A = 0.2$
- $K_A = 0.5$
- $K_A = 0.8$
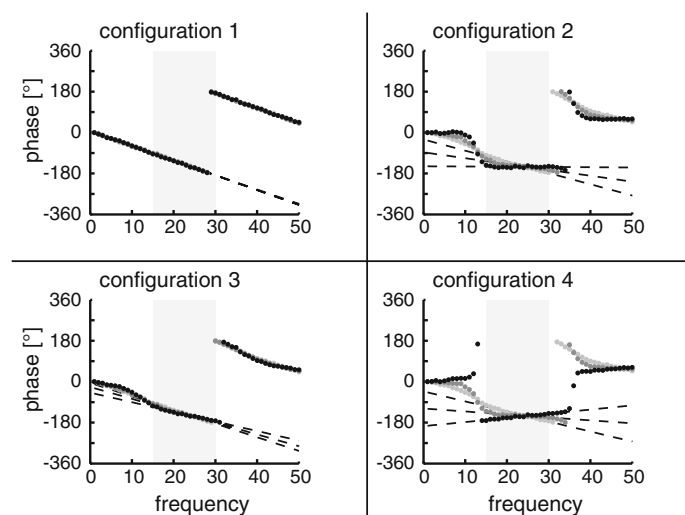
Fig. 3 Time delays estimated from coherency phase ($y_c \rightarrow y_m$) as a function of K_A for three combinations of input signal variances and α. *Dashed lines* indicate transmission delays of efferent pathway (18ms) and afferent pathway (−25ms)

efferent transmission delay, similar to what is reported from experiments.

In Fig. 3 the estimated time delay is shown as a function of K_A for the three combinations of σ_{MD}^2, σ_{MN}^2 and α. When sensory feedback was not recorded in the cortical signal and not fed back to the motor activity (configuration 1) the estimated time delay always equaled the efferent transmission delay. When the system formed a closed feedback loop (configuration 2) the estimated time delay decreased with increasing K_A but was not dependent on σ_{MD}^2 and σ_{MN}^2. Additional simulations (not shown) indicated that in this configuration the estimated time delay was determined by the total loop gain ($K_E \cdot K_A$) and not by the relative strengths of the pathways.
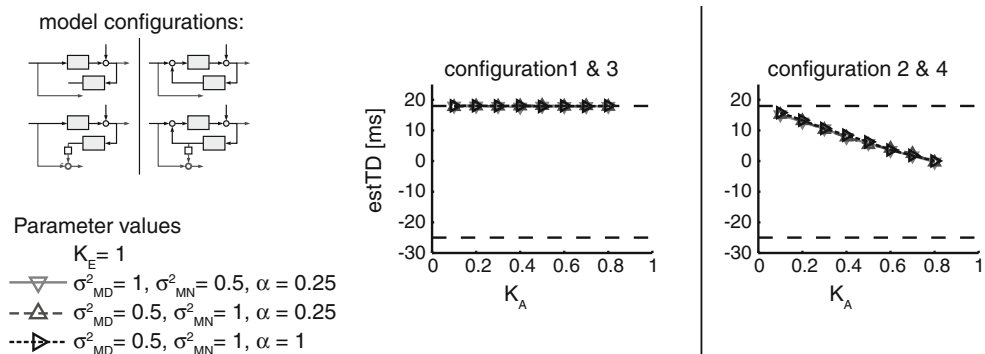
When sensory feedback was recorded in the cortical signal (configurations 3 and 4) the estimated time delay was affected by the total loop gain, the relative strengths of the pathways, the variances of the input signals and the contribution of the sensory feedback to the cortical signal. In these configurations the estimated time delay could even become negative for the largest values of K_A. The decrease of the estimated time delay with increasing K_A was even steeper when the variance of MN (σ_{MN}^2) increased relative the variance of MD (σ_{MD}^2) and when the contribution of SF to y_c

(α) increased. By manipulating the values of K_A, σ_{MN}^2, σ_{MD}^2 and α the estimated time delay can vary between the actual efferent and afferent transmission delays (not all combinations are shown). The estimated time delay in configuration 4 can be seen as a combination of the estimated time delays in configuration 2 and configuration 3 as there is the added effect of the closed loop feedback system (configuration 2) and the recording of sensory feedback in the cortical signal (configuration 3).
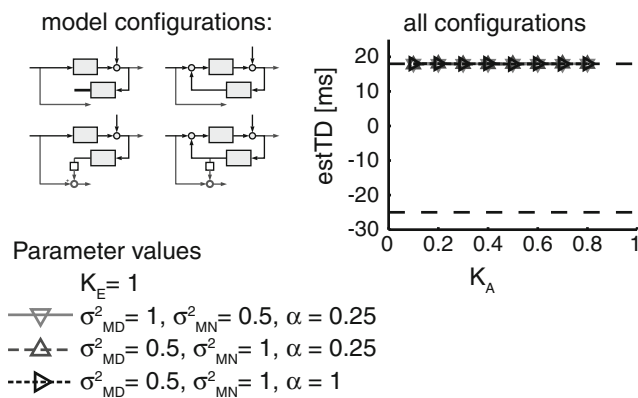
3.2 Directed connectivity time delay

The recording of the sensory feedback signal in the cortical signal did not influence the time delay estimated from DTF phase. However, a closed feedback loop configuration induced the same fluctuations in the phase frequency relation as were seen in the coherency phase. This again led to estimated time delays shorter than the efferent transmission delay (Fig. 4). Similar to what was seen when estimating the time delay from coherency phase in configuration 2, the estimated time delay decreased with increasing K_A but was not affected by the variances of the input signals nor the the contribution of sensory feedback to the cortical signal.

Fig. 4 Time delays estimated from DTF phase ($y_c \rightarrow y_m$) as a function of K_A for three combinations of input signal variances and α. Model configuration 1 and 3 and model configurations 2 and 4 gave the same time delay estimates. *Dashed lines* indicate transmission delays of efferent pathway (18ms) and afferent pathway (−25ms)

model configurations:

all configurations

Parameter values
$K_E = 1$
$\triangledown$ — $\sigma^2_{MD} = 1,\ \sigma^2_{MN} = 0.5,\ \alpha = 0.25$
$-\triangle-$ $\sigma^2_{MD} = 0.5,\ \sigma^2_{MN} = 1,\ \alpha = 0.25$
$\cdots\triangleright\cdots$ $\sigma^2_{MD} = 0.5,\ \sigma^2_{MN} = 1,\ \alpha = 1$

Fig. 5 Time delays estimated from PDC phase ($y_c \rightarrow y_m$) as a function of K_A for three combinations of input signal variances and α. All model configurations gave the same time delay estimates. Dashed lines indicate transmission delays of efferent pathway (18ms) and afferent pathway (-25ms)

The phase of PDC was proportional to frequency in all simulations and time delays estimated from PDC phase always equaled the efferent transmission delay (Fig. 5). There was no effect of the input signal variance nor of the contribution of sensory feedback to the cortical signal.

4 Discussion

In various fields of neuroscience, the coherency phase is interpreted in terms of a time delay between two signals and is used to disentangle the structure of functional networks between populations of neurons (Tallon-Baudry et al. 2001; Weiss and Mueller 2003; Riddle et al. 2004; Witham et al. 2007; Nolte et al. 2008; Williams et al. 2009). In the corticomuscular system, smaller than expected time delays are found between cortical (EEG or MEG) and muscle (EMG) signals (Halliday et al. 1998; Brown et al. 1998; Grosse et al. 2003; Riddle and Baker 2005). Although it is generally accepted that CMC arises due to bidirectional connectivity (Baker 2007), the effect of sensory feedback on CMC phase or directed connectivity measures has not been thoroughly investigated. We used a model representing the corticomuscular system to investigate how time delays estimated from coherency, DTF and PDC phase are affected by a closed feedback loop and the recording of sensory feedback in the cortical signal.

When transmission delays can be estimated reliably from connectivity measures this could provide information about which pathways, i.e. direct oligosynaptic pathways or indirect polysynaptic pathways, are actually in use during a task (Lindemann et al. 2001). This is opposed to using external stimuli to elicit responses which provide structural information about the which pathways are available between different parts of the (central) nervous system.

An important outcome of our simulations is that in a closed feedback loop without the recording of sensory feedback in the cortical signal (model configuration 2), the estimated time delays based on coherency were shorter than the transmission delay of the efferent pathway. This means that even when no bidirectional connectivity is detected because sensory feedback is not recorded, time delays estimated from coherency phase are potentially meaningless estimates of the neural transmission delay. When sensory feedback was recorded in the cortical signal, resulting in a bidirectional connectivity between cortical and muscle signal, a wide range of time delays was estimated from coherency phase depending on the model configuration, strength of the efferent and afferent pathways, the variances of the input signals and the magnitude of the sensory feedback in the cortical signal. The different time delay estimates result from the fluctuations in the phase frequency relation. With the physiologically realistic values for the efferent and afferent transmission delays, the fluctuations in the coherency phase cannot be seen in the beta band. The range of estimated positive and negative time delays based on the beta band was similar to the range of time delays reported from experiments in literature from CMC phase (Halliday et al. 1998; Brown et al. 1998; Gross et al. 2000; Grosse et al. 2003; Riddle and Baker 2005; Petersen et al. 2012). When estimating time delays based on different frequency bands, an even wider range of estimated time delays would have been obtained. However, in experimental studies, significant coherence is generally not found outside the beta band. Recent studies showed that there is a bidirectional relation between the EEG/MEG and the EMG and that there are indeed sensory components in the EEG measured over the motor cortex (Witham et al. 2011; Jain et al. 2012). The complex interplay between the different structures in the corticomuscular system, essentially makes it impossible to estimate transmission delays based on coherency phase in the corticomuscular system.

There are multiple techniques and measures available that include directionality in the estimation of connectivity which may identify properties of individual pathways in case of bidirectional connectivity. We included two measures based on Granger causality (Granger 1969) and a MVAR model of the data: the directed transfer function and partial directed coherence (Baccalá and Sameshima 2001; Kamiński and Blinowska 1991). Here we used these techniques to investigate a model representing corticomuscular connectivity. When the activity of multiple cortical areas can be directly measured by local field potentials or can be reliably reconstructed from scalp recordings, fitting of higher order MVAR models allows the study of connectivity between multiple cortical areas (Astolfi et al. 2007; Porcaro et al. 2013). However, care should be taken to avoid computational difficulties or the detection of spurious interaction

due to common sources and volume conduction (Haufe et al. 2013). Recently, directed coherence, which is similar to DTF (Baker et al. 2006), has been used assess directionality and pathway properties in the corticomuscular system (Witham et al. 2011). The results of Witham et al. (2011) confirmed the bidirectional connectivity between cortex and periphery during motor control.

In the bivariate case, DTF and PDC give the same results on the connectivity pattern, as long as $\overline{\mathbf{A}}(f)$ (Eq. (8)) is invertible (Baccalá and Sameshima 2001). In a MVAR model $\overline{\mathbf{A}}(f)$ can become ill-conditioned when signals have a common source, for example as a result of volume conduction between EEG channels. In addition to this computational disadvantage of the DTF, our results show that DTF and PDC are not equally suited to estimate transmission delays. Only the time delays estimated from PDC phase equaled the afferent transmission delay. The DTF phase resulted in estimated time delays shorter that the efferent transmission delays when the model formed a closed loop feedback system. The DTF represents the transfer function from the external noise sources to the recorded signals, in a closed loop feedback system these transfer functions include the dynamics of the entire loop (Schouten and Campfens 2012).

Partial directed coherence is directly based on the parameters of the MVAR model, describing the relation between past samples of the recorded signals and the current sample. In this way the dynamics of individual pathways can be captured. In our simulations, correct identification of the MVAR model was aided by the simple model structure, absence of measurement noise, white noise characteristics of the input signals (Ljung 1999) and no preprocessing of the recorded cortical and muscle activity (Florin et al. 2010). The dynamics of the pathways were solely determined by the transmission delays and therefore the resulting PDC phase had a proportional relation with frequency. This allowed correct estimation of the time delay even in a narrow frequency band. When a neural pathway contains more dynamics than a transmission delay alone, these dynamics will be seen in the PDC phase and affect the estimated time delay (Lindemann et al. 2001).

Clearly, the simulation model is a simplification of the complex physiology underlying motor control. However, the evaluated techniques implicitly assume such a simple system underlies the recorded signals. If techniques fail to reliably estimate transmission delays in our idealized simulations, these techniques will certainly fail when the true system is even more complex. We therefore advice against the use of coherence phase and DTF phase to estimate time delays when a closed feedback loop could underlie the recorded signals.

Partial Directed Coherence phase resulted in the correct estimation of transmission delays in our simple simulation model. Whether a time delay estimated based on PDC phase will equal the transmission delay in experimental data will depend on many factors. As stated before, all dynamics of the pathways will affect the PDC phase and estimated time delay. Furthermore, the efferent and afferent pathway can most likely not be characterized by a single time delay while there are multiple nested feedback loops present in the motor control system. Because these nested feedback loops cannot be observed from non-invasive recordings of cortical activity and muscle activity, the time delays that are estimated based on PDC phase will represent a lumped time delay.

References

Abbruzzese, G., Berardelli, A., Rothwell, J.C., Day, B.L., Marsden, C.D. (1985). Cerebral potentials and electromyographic responses evoked by stretch of wrist muscles in man. *Experimental Brain Research*, *58*, 544–551.

Akaike, H. (1971). Autoregressive model fitting for control. *Annals of the Institute of Statistical Mathematics*, *23*(2), 163–180.

Astolfi, L., Cincotti, F., Mattia, D., Marciani, M.G., Baccalá, L.A., de Vico Fallani, F., Salinari, S., Ursino, M., Zavaglia, M., Ding, L., Edgar, J.C., Miller, G.A., He, B., Babiloni, F. (2007). Comparison of different cortical connectivity estimators for high-resolution EEG recordings. *Human Brain Mapping*, *28*(2), 143–157.

Baccalá, L.A., & Sameshima, K. (2001). Partial directed coherence: a new concept in neural structure determination. *Biological Cybernetics*, *84*(6), 463–474.

Baker, S.N. (2007). Oscillatory interactions between sensorimotor cortex and the periphery. *Current Opinion in Neurobiology*, *17*(6), 649–655.

Baker, S.N., Chiu, M., Fetz, E.E. (2006). Afferent encoding of central oscillations in the monkey arm. *Journal of Neurophysiology*, *95*(6), 3904–3910.

Brown, P., Salenius, S., Rothwell, J.C., Hari, R. (1998). Cortical Correlate of the Piper Rhythm in Humans. *Journal of Neurophysiology*, *80*, 2911–2917.

Florin, E., Gross, J., Pfeifer, J., Fink, G.R., Timmermann, L. (2010). The effect of filtering on Granger causality based multivariate causality measures. *Neuroimage*, *50*, 577–588.

Fries, P. (2005). A mechanism for cognitive dynamics: neuronal communication through neuronal coherence. *Trends in Cognitive Sciences*, *9*(10), 474–480.

Granger, C. (1969). Investigating causal relations by econometric models and cross-spectral methods. *Econometrica*, *37*(3), 424–438.

Gross, J., Tass, P.A., Salenius, S., Hari, R., Freund, H.J., Schnitzler, A. (2000). Cortico-muscular synchronization during isometric muscle contraction in humans as revealed by magnetoencephalography. *Journal of Physiology*, *527*(Pt 3), 623–631.

Grosse, P., Guerrini, R., Parmeggiani, L., Bonanni, P., Pogosyan, A., Brown, P. (2003). Abnormal corticomuscular and intermuscular coupling in high-frequency rhythmic myoclonus. *Brain*, *126*(Pt 2), 326–342.

Halliday, D.M., Rosenberg, J.R., Amjad, A.M., Breeze, P., Conway, B.A., Farmer, S.F. (1995). A framework for the analysis of mixed time series/point process data–theory and application to the study

of physiological tremor, single motor unit discharges and electromyograms. *Progress in Biophysics and Molecular Biology*, *64*(2–3), 237–278.

Halliday, D.M., Conway, B.A., Farmer, S.F., Rosenberg, J.R. (1998). Using electroencephalography to study functional coupling between cortical activity and electromyograms during voluntary contractions in humans. *Neuroscience Letters*, *241*(1), 5–8.

Haufe, S., Nikulin, V.V., Müller, K.R., Nolte, G. (2013). A critical assessment of connectivity measures for EEG data: a simulation study. *NeuroImage*, *64*, 120–133.

Horwitz, B. (2003). The elusive concept of brain connectivity. *Neuroimage*, *19*(2 Pt 1), 466–470.

Jain, S., Gourab, K., Schindler-Ivens, S., Schmit, B.D. (2012). EEG during pedaling: evidence for cortical control of locomotor tasks. *Clinical Neurophysiology*.

Kamiński, M., & Blinowska, K.J. (1991). A new method of the description of the information flow in the brain structures. *Biological Cybernetics*, *65*(3), 203–210.

Lindemann, M., Raethjen, J., Timmer, J., Deuschl, G., Pfister, G. (2001). Delay estimation for cortico-peripheral relations. *Journal of Neuroscience Methods*, *111*(2), 127–139.

Ljung, L. (1999). System Identification: Theory for the users, 2nd ed. Prentice Hall PTR.

Mima, T., Steger, J., Schulman, A.E., Gerloff, C., Hallett, M. (2000). Electroencephalographic measurement of motor cortex control of muscle activity in humans. *Clinical Neurophysiology*, *111*(2), 326–337.

Mima, T., Matsuoka, T., Hallett, M. (2001). Information flow from the sensorimotor cortex to muscle in humans. *Clinical Neurophysiology*, *112*(1), 122–126.

Nolte, G., Bai, O., Wheaton, L., Mari, Z., Vorbach, S., Hallett, M. (2004). Identifying true brain interaction from EEG data using the imaginary part of coherency. *Clinical Neurophysiology*, *115*(10), 2292–2307.

Nolte, G., Ziehe, A., Nikulin, V.V., Schlögl, A., Krämer, N., Brismar, T., Müller, K.R. (2008). Robustly estimating the flow direction of information in complex physical systems. *Physical Review Letters*, *100*(23), 234–101.

Petersen, T.H., Willerslev-Olsen, M., Conway, B.A., Nielsen, J.B. (2012). The motor cortex drives the muscles during walking in human subjects. *Journal of Physiology*, *590*(Pt 10), 2443–2452.

Pintelon, R., & Schoukens, J. (2001). *System identification. A frequency domain approach*. Piscataway, NJ: IEEE Press.

Pohja, M., & Salenius, S. (2003). Modulation of cortex-muscle oscillatory interaction by ischaemia-induced deafferentation. *Neuroreport*, *14*(3), 321–324.

Porcaro, C., Coppola, G., Pierelli, F., Seri, S., Di Lorenzo, G., Tomasevic, L., Salustri, C., Tecchio, F. (2013). Multiple frequency functional connectivity in the hand somatosensory network: an EEG study. *Clinical Neurophysiology*, *124*(6), 1216–1224.

Riddle, C.N., & Baker, S.N. (2005). Manipulation of peripheral neural feedback loops alters human corticomuscular coherence. *Journal of Physiology*, *566*(Pt 2), 625–639.

Riddle, C.N., Baker, M.R., Baker, S.N. (2004). The effect of carbamazepine on human corticomuscular coherence. *Neuroimage*, *22*(1), 333–340.

Rosenberg, J.R., Amjad, A.M., Breeze, P., Brillinger, D.R., Halliday, D.M. (1989). The Fourier approach to the identification of functional coupling between neuronal spike trains. *Progress in Biophysics and Molecular Biology*, *53*(1), 1–31.

Rothwell, J.C., Thompson, P.D., Day, B.L., Boyd, S., Marsden, C.D. (1991). Stimulation of the human motor cortex through the scalp. *Experimental Physiology*, *76*, 159–200.

Schneider, T., & Neumaier, A. (2001). Algorithm 808: ARfit—a matlab package for the estimation of parameters and eigenmodes of multivariate autoregressive models. *ACM Transactions on Mathematical Software*, *27*(1), 58–65.

Schouten, A.C., & Campfens, S.F. (2012). Directional coherence disentangles causality within the sensorimotor loop, but cannot open the loop. *Journal of Physiology*, *590*(Pt 10), 2523–2529.

Stam, C.J., & van Straaten, E.C.W. (2012). The organization of physiological brain networks. *Clinical Neurophysiology*, *123*(6), 1067–1087.

Tallon-Baudry, C., Bertrand, O., Fischer, C. (2001). Oscillatory synchrony between human extrastriate areas during visual short-term memory maintenance. *Journal of Neuroscience*, *21*(20), RC177.

Varela, F., Lachaux, J.P., Rodriguez, E., Martinerie, J. (2001). The brainweb: phase synchronization and large-scale integration. *Nature Reviews Neuroscience*, *2*(4), 229–239.

Weiss, S., & Mueller, H.M. (2003). The contribution of EEG coherence to the investigation of language. *Brain and Language*, *85*(2), 325–343.

Williams, E.R., Soteropoulos, D.S., Baker, S.N. (2009). Coherence between motor cortical activity and peripheral discontinuities during slow finger movements. *Journal of Neurophysiology*, *102*(2), 1296–1309.

Witham, C.L., Wang, M., Baker, S.N. (2007). Cells in somatosensory areas show synchrony with beta oscillations in monkey motor cortex. *The European Journal of Neuroscience*, *26*(9), 2677–2686.

Witham, C.L., Riddle, C.N., Baker, M.R., Baker, S.N. (2011). Contributions of descending and ascending pathways to corticomuscular coherence in humans. *Journal of Physiology*, *589*(Pt 15), 3789–3800.